Construction and analysis of causally dynamic hybrid bond graphs

Rebecca Margetts, Roger F Ngwompo and Marcelin Fortes da Cruz

Proceedings of the Institution of Mechanical Engineers, Part I: Journal of Systems and Control Engineering 2013 227: 329
DOI: 10.1177/0959651812466530

Original Article

Institution of MECHANICAL ENGINEERS

Journal of SYSTEMS AND CONTROL ENGINEERING

Proc IMechE Part I:
J Systems and Control Engineering
227(3) 329–346

DOI: 10.1177/0959651812466530
pii.sagepub.com
SAGE

Construction and analysis of causally dynamic hybrid bond graphs

Rebecca Margetts[1], Roger F Ngwompo[1] and Marcelin Fortes da Cruz[2]

Abstract

Engineering systems are frequently abstracted to models with discontinuous behaviour (such as a switch or contact), and a hybrid model is one which contains continuous and discontinuous behaviours. Bond graphs are an established physical modelling method, but there are several methods for constructing switched or 'hybrid' bond graphs, developed for either qualitative 'structural' analysis or efficient numerical simulation of engineering systems. This article proposes a general hybrid bond graph suitable for both. The controlled junction is adopted as an intuitive way of modelling a discontinuity in the model structure. This element gives rise to 'dynamic causality' that is facilitated by a new bond graph notation. From this model, the junction structure and state equations are derived and compared to those obtained by existing methods. The proposed model includes all possible modes of operation and can be represented by a single set of equations. The controlled junctions manifest as Boolean variables in the matrices of coefficients. The method is more compact and intuitive than existing methods and dispenses with the need to derive various modes of operation from a given reference representation. Hence, a method has been developed, which can reach common usage and form a platform for further study.

Keywords

Physical system models, hybrid bond graphs, switched bond graphs, causality, junction structure, structural analysis, control

Date received: 29 June 2012; accepted: 9 October 2012

Introduction

Bond graphs are an established, well-documented method for mechatronic system modelling. Hybrid bond graphs – that is, bond graphs incorporating both continuous and discontinuous behaviour – are an area of active research. There are a number of proposed approaches to modelling discontinuities in bond graphs, and a substantial body of work has already been conducted. No one method for hybrid bond graphs has reached common usage. This article proposes a method for constructing hybrid bond graphs and generating equations from them, considering the issue of dynamic causality on commutation. The method can be used for both qualitative analysis and numerical simulation of applications, and it is anticipated that this approach can be adopted throughout the modelling community to facilitate further work on hybrid modelling.

Early attempts to model discontinuous behaviour yielded the time-dependent junction (tdj)[1] and the use of modulated resistance elements to represent hydraulic valves.[1,2] Subsequently, a number of methods for representing discontinuities in the bond graph were proposed, including the switching transformer element,[3] ideal switch[4] or switched source (sometimes known as a switched element),[5] controlled junction (similar in principle to the time dependent junction)[6] and switched storage element.[7] Other methods included using petri nets to link a selection of continuous-time models,[8] the quantised bond graph[9] (which is completely discrete and can be solved by discrete event simulation (DEVS)), and the impulse bond graph[10] (which explicitly considers impulses in variable structure systems). A full discussion of these methods is outside the scope of this article. Throughout the latter half of the 1990s, a body of work on the simulation of hybrid bond graph models was produced in which switched sources and controlled

[1]Department of Mechanical Engineering, University of Bath, Bath, UK
[2]Airbus Operations Ltd, Bristol, UK

Corresponding author:
Rebecca Margetts, Department of Mechanical Engineering, University of Bath, Claverton Down, Bath BA2 7AY, UK.
Email: R.Margetts@bath.ac.uk

junctions emerged as the key methods,[11–19] and these are still in usage.

Switched sources (which commutate between being an effort and a flow source) were used extensively in subsequent work on (bond-graph-based) structural analysis.[20–25] By rearranging the junction structure matrix (JSM) into an implicit form, a switching law can be included to describe the relationship between the switched source's input and output variables. A state equation for the reference mode of operation can be obtained from this, and other modes of operation derived in turn. However, switched sources have been criticised because a switch is a control element, not an energy processing element.[6,26]

The bulk of work on hybrid bond graphs for simulation used the controlled junction (which is a regular constant flow or effort junction when ON and a source of zero flow or effort when OFF).[27–33] Typically, a range of continuous models are produced, and a finite state automaton or transform in state space links them.

Some interesting variants on these methods have been proposed. Low et al.[34–36] produced a series of articles looking at hybrid bond graphs for fault detection and isolation (FDI) and defining a causality assignment procedure for hybrid bond graphs. Although they initially used switched sources, they adopted controlled junctions but used a subtly different version in which the junction is deleted when 'OFF'. There is also a switched power junction proposed by Umarikar and Umanand,[37] which has two mutually exclusive effort- or flow-deciding bonds (rather than being ON or OFF like a controlled junction). The rest of the bond graph remains in static causality.

A Boolean modulated transformer (MTF) connected to a resistance element can be used like a switched source, with the resistance modelling the internal resistance of the real switch.[38] This approach has been used most recently by Borutzky[39] who fixes the causality of the resistor and uses the resulting invariant causality bond graph for FDI (generating results comparable to those obtained by Low et al.). This gives a unique model covering all modes of operation, but with fixed causality.

Causality can be exploited and the junction structure can be inspected to reveal information about the model prior to numerical simulation (sometimes called 'structural analysis') in a manner corresponding to the structural analysis of the state matrices in control theory.[40–43] A feature of hybrid bond graphs is that the ideal causal assignment of the bond graph can change with commutation of the new switching parts. In some cases, this is due to the variable topology of the model, for example, two bodies contacting and coalescing. This idea of variable causality and topology has been addressed by several authors.[5,44,45] Much of the work conducted to date restricts dynamic causality by adding parasitic compliance or 'causality resistance'[4] or using novel causality assignments like hybrid sequential causality assignment procedure (Hybrid-SCAP).[35] This is intended to facilitate simulation, but can cause problems by creating an overly complex stiff model,[46] and is open to abuse (i.e. there is a danger that resistances may be added purely to aid computation with no consideration of the physical system). It may restrict insight into the model by breaking causal paths that would otherwise occur, and it may be undesirable to have extra small compliances or resistances in applications where a reduced-order 'proper model' is needed. It has been suggested that dynamic causality is preferable, revealing something of the model's properties.[45] However, authors who allow dynamic causality typically transfer the model to another software environment (where some kind of automaton or algebraic state mapping handles the discontinuity and state variables can be reinitialised after each transition), losing the graphical advantages of bond graphs.

This article makes a distinction between *structural discontinuities* (e.g. a physical switch, clutch or valve that connects or disconnects part of the model: often resulting in a variable topology model) and *parametric discontinuities* (e.g. an element with a highly non-linear behaviour, which can be abstracted to piecewise continuous relationships). The focus is on structural discontinuities in order to utilise the linear time-invariant (LTI) state space representation for the general model.

The purpose of this article is to create a hybrid bond graph that facilitates qualitative analysis and engineering insight, as well as being suitable for efficient simulation. It has the following features.

- The controlled junction was selected as an established method for showing discontinuities in a bond graph, which is the most intuitive method because it (dis)connects parts of the bond graph. This mirrors structural changes in topology that occur in the idealised physical system and therefore can be exploited to give insight into the system. In contrast, the switching source adds extra inputs and results in a switching law being added to the model equations in a form unsuitable for simulation.
- The equations derived from this graph are unique and represent all modes, with Boolean variables referring to an absolute OFF or ON state of each controlled junction. In contrast, the equations derived from systems with switching sources describe a reference model and switching laws enabling other modes of operation to be derived.
- Dynamic causality is allowed so as to give maximum insight into the model and prevent unwanted complexity and high frequency dynamics (which can occur in models where the causal assignment is kept static). This is shown on the bond graph, again to aid insight.

The causally dynamic hybrid bond graph

Use of the controlled junction in the hybrid bond graph

Structural switching activates or deactivates part of a system, for example, a physical switch, clutch or

hydraulic valve. A controlled junction can be used to (dis)connect or (de)activate part of the model accordingly. Controlled junctions, defined by Mosterman and Biswas,[14] are recommended by other authors[26,35] as an intuitive and physically correct representation for structural discontinuities because they clearly show where elements connect and disconnect and break the path of power flow.

A controlled junction behaves as a normal 1- or 0-junction when ON and a source of zero flow or effort (respectively) when OFF. A controlled 1-junction is therefore used to break or inhibit flow (e.g. an electrical switch that breaks the flow of current) and a controlled 0-junction is used to inhibit effort (e.g. a clutch or other physical non-contact in a mechanical system). This always gives rise to dynamic causality on one of the attached bonds. The commonly accepted notation for controlled junctions is X1 and X0, which will be used in this article.

Based on the above description, controlled junctions X1 and X0 can be formally defined as 2-port elements with associated Boolean parameters λ. The restriction to two ports is for practical reasons and the definition can easily be extended to more than two ports. Bond graph representations of controlled junctions X1 and X0 are shown in Figure 1, and their defining relationships are given by equations (1) and (2), respectively.

$$\begin{cases} \lambda f_1 = \lambda f_2 \\ \lambda (e_1 - e_2) = 0 \\ \bar{\lambda} f_1 = 0 \\ \bar{\lambda} f_2 = 0 \end{cases} \quad (1)$$

$$\begin{cases} \lambda e_1 = \lambda e_2 \\ \lambda (f_1 - f_2) = 0 \\ \bar{\lambda} e_1 = 0 \\ \bar{\lambda} e_2 = 0 \end{cases} \quad (2)$$

The Boolean parameter λ selects the set of equations that are valid given the state of the switch: $\lambda = 1$ when the switch is ON and $\lambda = 0$ when the switch is OFF. For each controlled junction, the above defining equations (1) and (2) lead to three possible causal configurations.

- Two causal configurations when the switch is ON, that is, $\lambda = 1$ (first two equations equivalent to a normal 1 or 0 junction).
- A unique causal configuration when the switch is OFF, that is, $\lambda = 0$ (last two equations equivalent to null sources of flow or null sources of effort imposed by the element to both power ports with conjugate variables externally imposed to the element).

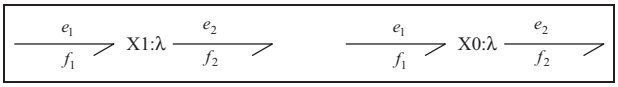

Figure 1. Bond graph representation of controlled junctions X1 and X0.

Controlled junction definitions, their possible causal configurations depending on the state of the switches and the associated assignment statements are summarised in Table 1. The formal definition of controlled junctions proposed here indicates that these elements are represented in terms of bond graph as elements 'switching' between standard 0- or 1-junctions and null sources. This appears to be a natural physical interpretation not shown by other representations using only null sources or MTFs with resistors.

A dynamic causality assignment procedure for the hybrid bond graph

Causality in a bond graph is typically assigned using the *Sequential Causality Assignment Procedure (SCAP)*.[47] There are some alternative causality assignment procedures for hybrid models aimed at efficient simulation and producing a causally static diagnostic hybrid bond graph. Using controlled junctions in the general case without parasitic resistive elements, dynamic causality is unavoidable. However, dynamic causality can be minimised (without artificially constraining it) in order to generate the smallest possible set of equations. Low et al.[35] observe that dynamic causality can be minimised when a 1-port element is on the junction. However, their assertion that static causality can be maintained only applies to their method of deleting the controlled junction when it is OFF, potentially giving rise to hanging junctions/elements and a different causality assignment (see Figure 2).

The causality assignment procedure for hybrid bond graphs proposed in this study starts with a reference mode of operation defined with a maximum number of elements in integral causality and controlled junctions preferably ON. This is the mode that should be easiest to simulate. Deviations from this reference due to dynamic causality are marked as dashed causal strokes. This enables the user to see the effects of commutation on causality and aids in equation generation. The dynamic sequential causality assignment procedure (DSCAP) to represent all modes of a hybrid bond graph model can be summarised in the following procedure.

DSCAP for hybrid bond graph.

Step 1. Assign causality according to SCAP with preferred integral causality, stopping when a controlled junction is reached, that is, start by assigning causality to a source element and propagate causality throughout the bond graph as far as any controlled junctions. Repeat for other source elements and then for any storage elements that have not yet been assigned causality. If causal conflict occurs in this stage, the model should be changed.

The causal assignment from step 1 may dictate whether some switches are ON or OFF.

Step 2. Choose a controlled junction that does not have its causality fully assigned. Assign causality around the

Table 1. Definition, causal configuration and equations of controlled junctions.

Controlled junction representation and defining equations	State of the switch	Possible causal configurations	Associated assignment statements
$\xrightarrow[f_1]{e_1}$ X1:λ $\xrightarrow[f_2]{e_2}$ $\begin{cases} \lambda f_1 = \lambda f_2 \\ \lambda (e_1 - e_2) = 0 \\ \bar{\lambda} f_1 = 0 \\ \bar{\lambda} f_2 = 0 \end{cases}$	ON (λ = 1)	$\vdash\xrightarrow[f_1]{e_1}$ X1:λ $\vdash\xrightarrow[f_2]{e_2}$	$e_1 := e_2$ $f_2 := f_1$
		or	or
		$\xrightarrow[f_1]{e_1}\vert$ X1:λ $\vert\xrightarrow[f_2]{e_2}$	$e_2 := e_1$ $f_1 := f_2$
	OFF (λ = 0)	$\xrightarrow[f_1]{e_1}\vert$ X1:λ $\vert\xrightarrow[f_2]{e_2}$	$f_1 := 0$ $f_2 := 0$ e_1 and e_2 arbitrary
$\xrightarrow[f_1]{e_1}$ X0:λ $\xrightarrow[f_2]{e_2}$ $\begin{cases} \lambda e_1 = \lambda e_2 \\ \lambda (f_1 - f_2) = 0 \\ \bar{\lambda} e_1 = 0 \\ \bar{\lambda} e_2 = 0 \end{cases}$	ON (λ = 1)	$\vdash\xrightarrow[f_1]{e_1}$ X0:λ $\vdash\xrightarrow[f_2]{e_2}$	$e_2 := e_1$ $f_1 := f_2$
		or	or
		$\xrightarrow[f_1]{e_1}\vert$ X0:λ $\vert\xrightarrow[f_2]{e_2}$	$e_1 := e_2$ $f_2 := f_1$
	OFF (λ = 0)	$\vdash\xrightarrow[f_1]{e_1}$ X0:λ $\vert\xrightarrow[f_2]{e_2}$	$e_1 := 0$ $e_2 := 0$ f_1 and f_2 arbitrary

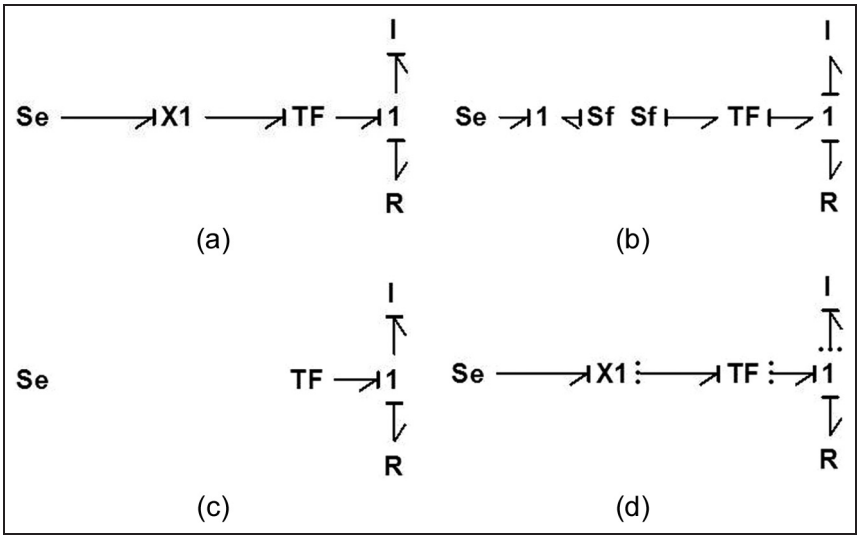

Figure 2. An example of causality assignment and their effect around a controlled junction: (a) the junction in the ON (reference) mode, (b) the junction shown by null sources in the OFF position, (c) the causality assignment gained when the switch is deleted in the OFF position (I remains in integral causality) as proposed by Low et al.[35] and (d) the proposed method for showing dynamic causality.

controlled junctions assuming the switch to be ON (as indicated in Table 1) and propagate as far as possible. Repeat this stage until all the controlled junctions have their causality fully assigned.

Step 3. Finish propagating causality throughout the bond graph to any resistance elements or remaining bonds and propagate as far as possible.

Step 4. Taking each controlled junction in turn, consider the causality assignment when it is in the other state to the reference configuration. Mark this causality assignment with a dashed causal stroke and propagate throughout the bond graph (Figure 2(d)). If causal conflict occurs in this stage, then the other state of the controlled junction is not allowed.

Remark. Causal propagations in step 2 and step 4 of the algorithm above may dictate the state (ON or OFF) of some controlled junctions as a result of the assigned state of others. This reveals some constraints in the state of switches indicating the allowed configurations or physically feasible modes of operation.

Figure 2 shows a simple example of the effect of the causality assignment around a controlled junction when ON and OFF. The representation is compared in this example with the method of deleting the switch when OFF as proposed by Low et al.[35]

Equation generation from dynamic causal bond graphs

The terms in the underlying equations change when causality is dynamic. Storage elements may switch from integral to derivative causality, and the inputs and outputs of the resistance elements may reverse. The resulting state space matrices may change size depending on the mode. Sueur and Dauphin-Tanguy[48] suggest the use of a 'pseudo-state variable' when analysing models with elements in derivative causality. This is not a conventional state variable, but the input to the junction structure from an element in derivative causality. When it is included in the equations it generates an algebraic equation that relates to the other state equations.

Storage elements in dynamic causality can be described using a variable for each of the two possible causal assignments: a state variable for the integral causality case, and a 'pseudo-state variable' for derivative causality. Buisson et al.[20] do this to recover the implicit state equations from a single mode of operation. The philosophy of using two variables, a state and a 'pseudo-state', to represent the two modes of storage element can be extended here. In this article, an implicit model is presented, which describes all possible modes of operation. Multiple variables are used to describe elements in dynamic causality, which are (de)activated in the appropriate modes of operation. The LTI form remains valid because the switching behaviour is not necessarily a function of time: the equations capture the model at all time points.

Implicit formulation of the hybrid junction structure relation

The general hybrid bond graph

A causal bond graph model can be represented in matrix format, as a JSM consisting of ones and zeros that relate the system inputs and outputs. The JSM based on the Paynter junction structure is used here since it has reached common use in bond graph structural analysis. The coefficients in the transformer field (representing any transformer or gyrator elements, sometimes expressed outside the JSM) are brought inside the JSM to give terms other than one and zero.

The general bond graph structure is shown in Figure 2, with a modified 'hybrid' version to capture structural switching behaviour and the induced dynamic causality. Using the DSCAP proposed above, the resulting hybrid causal bond graph would display some elements with static causality and some with dynamic causality represented by dashed causal strokes (Figure 2(b)). The hybrid junction structure matrix (HJSM; relating system inputs and outputs) and implicit state equation can be derived from this representation. For the general hybrid bond graph, the matrix $\mathbf{S}$ contains Boolean parameters λ indicating the state of controlled junctions. Switching terms in the sub-matrices of $\mathbf{S}$ will therefore be carried through into the state equations derived from it.

Figure 3 represents the block diagram derived from the hybrid causal bond graph, and the key variables used are defined as follows.

1. Elements with static causality have the usually defined variables.
   - Input vectors, denoted $\dot{\hat{\boldsymbol{X}}}_i$ (composed of $\dot{p}$ and $\dot{q}$ on I and C elements in integral causality), $\hat{\boldsymbol{Z}}_d$ (composed of f and e on I and C elements in derivative causality) and $\hat{\boldsymbol{D}}_{out}$ (composed of effort or flow variables into dissipative elements).
   - Output vectors denoted $\hat{\boldsymbol{Z}}_i$ and $\hat{\boldsymbol{X}}_i$ for storage elements and $\hat{\boldsymbol{D}}_{in}$ for dissipative elements.
2. However, dynamic causality is captured in the block diagram by specifying additional input and output variables. In any single mode of operation, one input and one output are active, and the others are redundant.
   - Two input vectors $\dot{\tilde{\boldsymbol{X}}}_i$ and $\tilde{\boldsymbol{Z}}_d$ composed of $\dot{p}$, $\dot{q}$, f and e for storage elements in dynamic causality $\tilde{\boldsymbol{D}}_{out} = \begin{bmatrix} \tilde{\boldsymbol{D}}_{e\_out} & \tilde{\boldsymbol{D}}_{f\_out} \end{bmatrix}^{\mathrm{T}}$ and composed of all effort and flow variables for dissipative elements in dynamic causality.
   - Two output vectors $\dot{\tilde{\boldsymbol{X}}}_d$ and $\tilde{\boldsymbol{Z}}_i$ composed of $\dot{p}$, $\dot{q}$, f and e for storage elements in dynamic causality $\tilde{\boldsymbol{D}}_{in} = \begin{bmatrix} \tilde{\boldsymbol{D}}_{e\_in} & \tilde{\boldsymbol{D}}_{f\_in} \end{bmatrix}^{\mathrm{T}}$ and composed of all effort and flow variables for dissipative elements in dynamic causality.

For elements with dynamic causality, the set of outputs is identical to the set of input variables with the difference in notation highlighted for practical reasons. Also, it is worth noting that an element can only have two modes of operation (flow input/effort output and effort input/flow output), although a model can have several modes of operation overall if it contains multiple controlled junctions.

The HJSM contains Boolean variables λ in addition to ones and zeros. Controlled junctions in the bond graph are assigned Boolean variables λ in the junction structure (which has a value of 1 when the junction is ON and 0 when OFF), signifying that there is a connection between two quantities when the junction is ON. A single bond graph therefore represents all possible modes of operation and causal assignments. Vectors

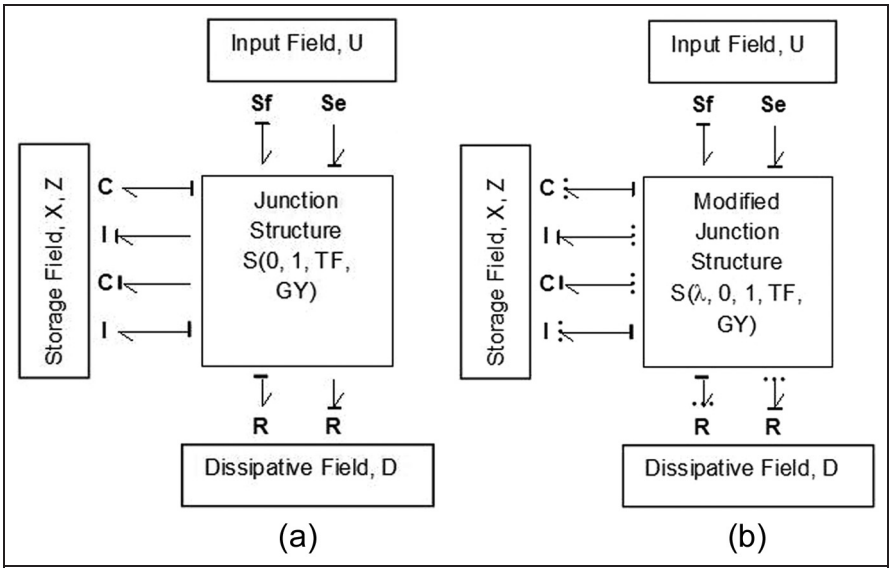

Figure 3. The junction structure matrix and generalised bond graph: (a) general junction structure and (b) hybrid junction structure incorporating switching (λ) coefficients and dynamic causality.

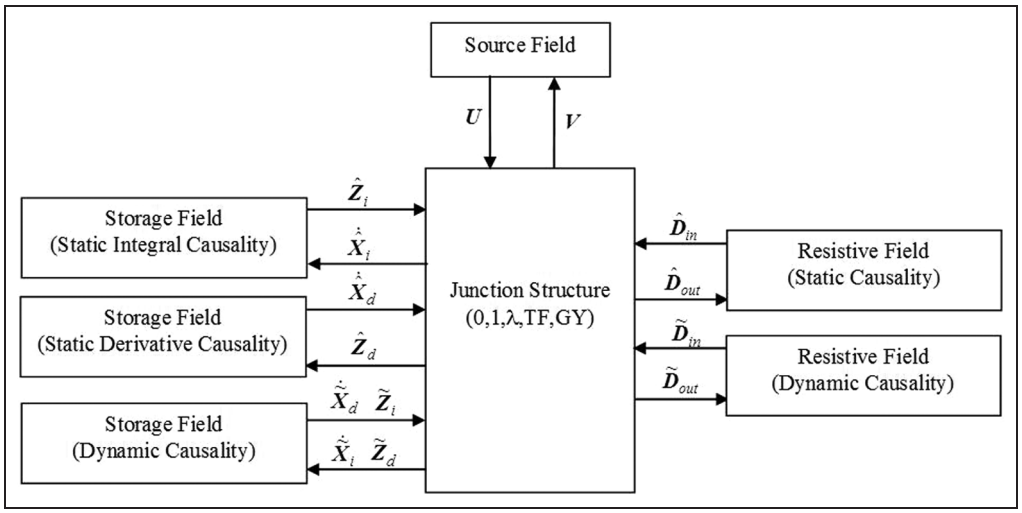

Figure 4. Quantities used in hybrid junction structure matrix and subsequent development.

$\dot{\boldsymbol{X}}_i = [\dot{\hat{\boldsymbol{X}}}_i \quad \dot{\tilde{\boldsymbol{X}}}_i]^{\mathrm{T}}$ and $\dot{\boldsymbol{X}}_d = [\dot{\hat{\boldsymbol{X}}}_d \quad \dot{\tilde{\boldsymbol{X}}}_d]^{\mathrm{T}}$ are the state and pseudo-state of the storage fields in integral and derivative causalities, respectively. $\boldsymbol{Z}_i = [\hat{\boldsymbol{Z}}_i \quad \tilde{\boldsymbol{Z}}_i]^{\mathrm{T}}$ and $\boldsymbol{Z}_d = [\hat{\boldsymbol{Z}}_d \quad \tilde{\boldsymbol{Z}}_d]^{\mathrm{T}}$ are the complementary vectors of these states (as shown in Figure 3), related by $\boldsymbol{Z}_i = \mathbf{F}_i \boldsymbol{X}_i$ and $\boldsymbol{Z}_d = \mathbf{F}_d \boldsymbol{X}_d$. The resistive field also has inputs $\boldsymbol{D}_{in} = [\hat{\boldsymbol{D}}_{in} \quad \tilde{\boldsymbol{D}}_{in}]^{\mathrm{T}}$ and outputs $\boldsymbol{D}_{out} = [\hat{\boldsymbol{D}}_{out} \quad \tilde{\boldsymbol{D}}_{out}]^{\mathrm{T}}$ and is related by $\boldsymbol{D}_{in} = \mathbf{L}\,\boldsymbol{D}_{out}$ (Figure 4).

Comparison of standard and hybrid model equations

The process of deriving a JSM, and then an implicit state equation, from a standard bond graph is well established,[41] as is the process for equation generation from a bond graph using switched sources.[20,23,41] For the hybrid bond graph (with controlled junctions) defined here, a similar procedure is followed with two important differences: the matrices obtained are functions of Boolean variables representing the controlled junctions parameters, and there is an additional matrix $\boldsymbol{\Lambda}(\lambda)$ that (de)activates outputs (i.e. multiplies them by zero or one) depending on whether they occur in a given mode of operation (Table 2). A single set of state equations is generated, which encompasses all possible modes of operation and caters for dynamic causality.

Remark. Although the input and output vectors of the junction structure for both the standard bond graph and the hybrid bond graph in the concatenated form junction look similar, the difference in the dimensions

Table 2. Junction structure and state space matrices forms for the standard and hybrid bond graphs.

	Standard bond graph	Hybrid bond graph with dynamic causality
Junction structure	$\begin{bmatrix} \dot{\boldsymbol{X}}_i \\ \boldsymbol{Z}_d \\ \boldsymbol{D}_{out} \end{bmatrix} = [\mathbf{S}(0, 1, \mathrm{TF}, \mathrm{GY})] \begin{bmatrix} \boldsymbol{Z}_i \\ \dot{\boldsymbol{X}}_d \\ \boldsymbol{D}_{in} \\ \boldsymbol{U} \end{bmatrix}$	$\boldsymbol{\Lambda}(\boldsymbol{\lambda}) \begin{bmatrix} \begin{bmatrix} \dot{\hat{\boldsymbol{X}}}_i \\ \dot{\tilde{\boldsymbol{X}}}_i \end{bmatrix} \\ \begin{bmatrix} \hat{\boldsymbol{Z}}_d \\ \tilde{\boldsymbol{Z}}_d \end{bmatrix} \\ \begin{bmatrix} \hat{\boldsymbol{D}}_{out} \\ \tilde{\boldsymbol{D}}_{out} \end{bmatrix} \end{bmatrix} = [\mathbf{S}(0, 1, \lambda, \mathrm{TF}, \mathrm{GY})] \begin{bmatrix} \begin{bmatrix} \hat{\boldsymbol{Z}}_i \\ \tilde{\boldsymbol{Z}}_i \end{bmatrix} \\ \begin{bmatrix} \dot{\hat{\boldsymbol{X}}}_d \\ \dot{\tilde{\boldsymbol{X}}}_d \end{bmatrix} \\ \begin{bmatrix} \hat{\boldsymbol{D}}_{in} \\ \tilde{\boldsymbol{D}}_{in} \end{bmatrix} \\ \boldsymbol{U} \end{bmatrix},$ which can be concatenated into $\boldsymbol{\Lambda}(\boldsymbol{\lambda}) \begin{bmatrix} \dot{\boldsymbol{X}}_i \\ \boldsymbol{Z}_d \\ \boldsymbol{D}_{out} \end{bmatrix} = [\mathbf{S}(0, 1, \lambda, \mathrm{TF}, \mathrm{GY})] \begin{bmatrix} \boldsymbol{Z}_i \\ \dot{\boldsymbol{X}}_d \\ \boldsymbol{D}_{in} \\ \boldsymbol{U} \end{bmatrix}$
Implicit state space equation	$\mathbf{E}\dot{\boldsymbol{X}} = \mathbf{A}\boldsymbol{X} + \mathbf{B}\boldsymbol{U}$	$\mathbf{E}(\boldsymbol{\Lambda})\dot{\boldsymbol{X}} = \mathbf{A}(\boldsymbol{\Lambda})\boldsymbol{X} + \mathbf{B}(\boldsymbol{\Lambda})\boldsymbol{U}$ with $\boldsymbol{\Lambda} = \mathbf{f}(\lambda_1, \lambda_2, \ldots \lambda_n)$. Hence, modes of operation are given by $\mathbf{E}(\boldsymbol{\Lambda}_1)\dot{\boldsymbol{X}} = \mathbf{A}(\boldsymbol{\Lambda}_1)\boldsymbol{X} + \mathbf{B}(\boldsymbol{\Lambda}_1)\boldsymbol{U}$ $\mathbf{E}(\boldsymbol{\Lambda}_2)\dot{\boldsymbol{X}} = \mathbf{A}(\boldsymbol{\Lambda}_2)\boldsymbol{X} + \mathbf{B}(\boldsymbol{\Lambda}_2)\boldsymbol{U}$ $\vdots$

should be noted. For the standard bond graph, $\dim \begin{bmatrix} \dot{\boldsymbol{X}}_i & \boldsymbol{Z}_d & \boldsymbol{D}_{out} \end{bmatrix}^{\mathrm{T}} = n_{\mathrm{IC}} + n_R$, and for the hybrid bond graph,$\dim \begin{bmatrix} \dot{\boldsymbol{X}}_i & \boldsymbol{Z}_d & \boldsymbol{D}_{out} \end{bmatrix}^{\mathrm{T}} = n_{\mathrm{IC}} + n_{\mathrm{R}} + n_{dyn}$, where n_{IC} is the number of storage elements, n_{R} is the number of dissipative elements and n_{dyn} is the number of elements with dynamic causality. Similar remarks can be made for the input vector.

Here, it will be assumed that the system elements are linear. If the LTI state space representation is derived from the JSM, the Boolean factors λ naturally appear in the **A** and **B** matrices of the state equations, as shown in Table 2. The LTI model is frequently used because no time is associated with the structural switching: it is simply acknowledged that there are different modes of operation. Note that this development assumes that each element has a linear, continuous constituent equation.

HJSM

As shown in section 'The general hybrid bond graph', there is one input and one output variable for each 1-port element in static causality. There are two inputs and two outputs for each 1-port element in dynamic causality. Both sets of input/output are exclusive of each other, and the Boolean terms in the HJSM will activate one of these for each mode of operation.

In order to establish which outputs of the junction structure are active, the vector of outputs must be multiplied by a diagonal matrix of Boolean expressions $\boldsymbol{\Lambda}(\boldsymbol{\lambda})$. In any one mode of operation, some rows of the matrices will be set to zeros and others will give the junction structure for that mode. Therefore, outputs that are in static causality are assigned a '1' in the diagonal of the matrix $\boldsymbol{\Lambda}(\boldsymbol{\lambda})$ because they are fixed outputs, while variables associated with elements in dynamic causality are assigned a Boolean function $f(\boldsymbol{\lambda})$ determined by the combination of the switch parameters λ that dictates the output status of the variable. For each Boolean term $f(\boldsymbol{\lambda})$, there will always be a NOT term $\overline{f(\boldsymbol{\lambda})}$ present in the matrix $\boldsymbol{\Lambda}(\boldsymbol{\lambda})$, which describes the dynamic element behaviour when the power variables switch from output to input or vice versa depending on the Boolean operations on the switch parameters being TRUE or FALSE.

In order to construct the matrix $\boldsymbol{\Lambda}(\boldsymbol{\lambda})$, consider each 1-port element in dynamic causality in turn, determine any causal paths between this elements and the controlled junctions and report the state of the switch and the output variable in a truth table. The truth table can therefore be used to construct the combination of states, and hence function of Boolean variables, that result in each causal change. For example, if a storage element is in integral causality only when two switches are ON, this could be expressed by assigning the state variable a term in $\boldsymbol{\Lambda}(\boldsymbol{\lambda})$ of $(\lambda_1 \bullet \lambda_2)$, that is, switch 1 AND switch 2 are true or ON (Table 3). The pseudo-state complementary variable Z_d would therefore be assigned $\overline{(\lambda_1 \bullet \lambda_2)}$ because the element is in derivative causality when switch 1 AND switch 2 are NOT true or OFF. Often, a controlled junction simply creates a path of dynamic causality between it and a nearby element, and the term in $\boldsymbol{\Lambda}(\boldsymbol{\lambda})$ can be quickly and easily assessed. There is the potential to reduce the amount of work required to obtain the equations by modularising and reusing sub-models for larger systems.

Table 3. Example truth table for two switches.

Switch 1	Switch 2	Causality on 1-port element	Output variable	Associated term in $\mathbf{\Lambda(\lambda)}$
0	0	Derivative	Z_d	$\overline{(\lambda_1 \bullet \lambda_2)}$
0	1	Derivative		
1	0	Derivative		
1	1	Integral	$\dot{X}_i$	$(\lambda_1 \bullet \lambda_2)$

The $\mathbf{S}$ matrix is constructed in the same way as for a regular bond graph, by considering which inputs give each output (assigning a 1 to true relationship and a 0 otherwise). Where the path between input and output crosses a controlled junction, a Boolean term λ expresses that the relationship holds true when that junction is ON (or OFF). In systems with more than one controlled junction, some of the Boolean expressions derived for $\mathbf{\Lambda(\lambda)}$ may need to be reused to reflect that inputs to each element may change with dynamic causality. Output of the hybrid dynamic junction structure can therefore be related to the input by equation (3)

$$\mathbf{\Lambda}(\lambda)\begin{bmatrix}\dot{\boldsymbol{X}}_i\\ \boldsymbol{Z}_d\\ \boldsymbol{D}_{out}\end{bmatrix} = \begin{bmatrix}\mathbf{S}_{11}(\lambda) & \mathbf{S}_{12}(\lambda) & \mathbf{S}_{13}(\lambda) & \mathbf{S}_{14}(\lambda)\\ -\mathbf{S}_{12}^{\mathrm{T}}(\lambda) & \mathbf{0} & \mathbf{0} & \mathbf{S}_{24}(\lambda)\\ -\mathbf{S}_{13}^{\mathrm{T}}(\lambda) & \mathbf{0} & \mathbf{S}_{33}(\lambda) & \mathbf{S}_{34}(\lambda)\end{bmatrix}\begin{bmatrix}\boldsymbol{Z}_i\\ \dot{\boldsymbol{X}}_d\\ \boldsymbol{D}_{in}\\ \boldsymbol{U}\end{bmatrix} \quad (3)$$

where the matrices $\mathbf{\Lambda}(\boldsymbol{\lambda})$ and $\mathbf{S}_{ij}(\boldsymbol{\lambda})$ are functions of the controlled junctions' Boolean parameters $\boldsymbol{\lambda}$. To simplify the notations, these matrices will simply be denoted as $\mathbf{\Lambda}$ and $\mathbf{S}_{ij}$ from this point forwards.

The $\mathbf{S}$ matrix in equation (3) is simplified since some properties always hold.

- The matrix is skew-symmetric, so $\mathbf{S_{21}}$ and $\mathbf{S_{31}}$ are equal to minus the transposes of $\mathbf{S_{12}}$ and $\mathbf{S_{13}}$. This is because of duality. Bonds represent power as the sum of flow and effort: if the flow input of one element is the flow output of another, then the efforts must also be connected.
- The complementary variable of the input (which would give row 4) can be ignored.
- When preferred integral causality is assigned, there can be no relation between the derivative causality and resistor fields, because this would imply a causal path that could be inverted to give integral causality.[20] There is also no relation between the derivative field and itself for the same reason. Hence, $\mathbf{S_{22}}$, $\mathbf{S_{23}}$ and $\mathbf{S_{32}}$ are all $\mathbf{0}$.

Note that $\mathbf{\Lambda}$ only needs to be applied to the left side of the equation because the terms in the JSM have been found by inspecting the causal paths in the model and therefore already contain Boolean values where needed.

A note on the reference configuration and other configurations

A reference configuration has been used to aid the construction of the causally dynamic bond graph and to act as a basis for the proposed dynamic causality notation. However, the JSM encapsulates all possible modes of operation and it is of little consequence which mode is selected for the reference. This is in contrast to previous work on bond graphs with switched sources,[20] which gives a JSM for a given reference mode, and other modes of operation are to be derived from it. As a consequence, other ideal approaches define the state of switches in each mode of operation relative to the reference mode (i.e. if λ is the parameter associated to a switch, then $\lambda = 1$ if the switch has commutated with respect to the reference configuration and $\lambda = 0$ otherwise), whereas the present approach suggests that the parameter λ of a switch indicates the absolute state of the switch, that is, $\lambda = 1$ when the switch is ON and $\lambda = 0$ when the switch is OFF.

The use of a controlled junction to (dis)connect parts of a bond graph dictates how discontinuous behaviour is abstracted and ensures conservation of momentum. The implications of this for simulation are a topic of further study.

Unique hybrid implicit state space equation

The state equations express the time derivatives of the states and (in this case) the pseudo-states – $\dot{\boldsymbol{X}}_i$ and $\dot{\boldsymbol{X}}_d$ – in terms of their integrals, and the system inputs $\boldsymbol{U}$. They can be derived from the JSM using the following procedure.

Equation (3) can be written with an appropriate partitioning of the diagonal matrix $\mathbf{\Lambda}$

$$\begin{bmatrix}\mathbf{\Lambda}_{11} & \mathbf{0} & \mathbf{0}\\ \mathbf{0} & \mathbf{\Lambda}_{22} & \mathbf{0}\\ \mathbf{0} & \mathbf{0} & \mathbf{\Lambda}_{33}\end{bmatrix}\begin{bmatrix}\dot{\boldsymbol{X}}_i\\ \boldsymbol{Z}_d\\ \boldsymbol{D}_{out}\end{bmatrix} = \begin{bmatrix}\mathbf{S}_{11} & \mathbf{S}_{12} & \mathbf{S}_{13} & \mathbf{S}_{14}\\ -\mathbf{S}_{12}^{\mathrm{T}} & \mathbf{0} & \mathbf{0} & \mathbf{S}_{24}\\ -\mathbf{S}_{13}^{\mathrm{T}} & \mathbf{0} & \mathbf{S}_{33} & \mathbf{S}_{34}\end{bmatrix}\begin{bmatrix}\boldsymbol{Z}_i\\ \dot{\boldsymbol{X}}_d\\ \boldsymbol{D}_{in}\\ \boldsymbol{U}\end{bmatrix} \quad (4)$$

Looking at row 3 of equation (4), an expression for $\boldsymbol{D}_{in}$ in terms of the other elements in the system can be derived

$$\boldsymbol{\Lambda}_{33}\boldsymbol{D}_{out} = -\mathbf{S}_{13}^{\mathrm{T}}\boldsymbol{Z}_i + \mathbf{S}_{33}\boldsymbol{D}_{in} + \mathbf{S}_{34}\boldsymbol{U} \tag{5}$$

where the constitutive equation for the dissipative field is

$$\boldsymbol{D}_{in} = \mathbf{L}\,\boldsymbol{D}_{out} \tag{6}$$

Substituting equation (6) into equation (5) and solving for $\boldsymbol{D}_{in}$ gives

$$\boldsymbol{D}_{in} = \mathbf{L}\left(\boldsymbol{\Lambda}_{33} - \mathbf{S}_{33}\mathbf{L}\right)^{-1}\left(-\mathbf{S}_{13}^{\mathrm{T}}\boldsymbol{Z}_i + \mathbf{S}_{34}\boldsymbol{U}\right) \tag{7}$$

Hence, the $\boldsymbol{D}_{in}$ terms can be eliminated from the system equations. Starting with row 1 of equation (4) for $\dot{\boldsymbol{X}}_i$

$$\begin{aligned}\boldsymbol{\Lambda}_{11}\dot{\boldsymbol{X}}_i = {} & \mathbf{S}_{11}\boldsymbol{Z}_i + \mathbf{S}_{12}\dot{\boldsymbol{X}}_d \\ & + \mathbf{S}_{13}\mathbf{L}\left(\boldsymbol{\Lambda}_{33} - \mathbf{S}_{33}\mathbf{L}\right)^{-1}\left(-\mathbf{S}_{13}^{\mathrm{T}}\boldsymbol{Z}_i + \mathbf{S}_{34}\boldsymbol{U}\right) + \mathbf{S}_{14}\boldsymbol{U}\end{aligned} \tag{8}$$

Defining $\mathbf{H} = \mathbf{L}\left(\boldsymbol{\Lambda}_{33} - \mathbf{S}_{33}\mathbf{L}\right)^{-1}$ allows equation (8) to be written in the following form

$$\begin{aligned}\boldsymbol{\Lambda}_{11}\dot{\boldsymbol{X}}_i = {} & \left(\mathbf{S}_{11} - \mathbf{S}_{13}\mathbf{H}\,\mathbf{S}_{13}^{\mathrm{T}}\right)\boldsymbol{Z}_i + \mathbf{S}_{12}\dot{\boldsymbol{X}}_d \\ & + \left(\mathbf{S}_{13}\mathbf{H}\,\mathbf{S}_{34} + \mathbf{S}_{14}\right)\boldsymbol{U}\end{aligned} \tag{9}$$

Combining equation (9) and row 2 of equation (4) leads to the following equation

$$\begin{aligned}&\begin{bmatrix}\boldsymbol{\Lambda}_{11} & -\mathbf{S}_{12}\\ \mathbf{0} & \mathbf{0}\end{bmatrix}\begin{bmatrix}\dot{\boldsymbol{X}}_i\\ \dot{\boldsymbol{X}}_d\end{bmatrix} \\ &= \begin{bmatrix}\mathbf{S}_{11} - \mathbf{S}_{13}\mathbf{H}\,\mathbf{S}_{13}^{\mathrm{T}} & \mathbf{0} & \mathbf{S}_{13}\mathbf{H}\,\mathbf{S}_{34} + \mathbf{S}_{14}\\ \mathbf{S}_{12}^{\mathrm{T}} & -\boldsymbol{\Lambda}_{22} & \mathbf{S}_{24}\end{bmatrix}\begin{bmatrix}\boldsymbol{Z}_i\\ \boldsymbol{Z}_d\\ \boldsymbol{U}\end{bmatrix}\end{aligned} \tag{10}$$

The complementary state variables can also be eliminated by considering the constitutive law for the storage elements

$$\begin{bmatrix}\boldsymbol{Z}_i\\ \boldsymbol{Z}_d\end{bmatrix} = \begin{bmatrix}\mathbf{F}_i & \mathbf{F}\\ \mathbf{F}^{\mathrm{T}} & \mathbf{F}_d\end{bmatrix}\begin{bmatrix}\boldsymbol{X}_i\\ \boldsymbol{X}_d\end{bmatrix} \tag{11}$$

Substituting equation (11) into equation (10) leads to the general implicit state equation

$$\begin{aligned}&\begin{bmatrix}\boldsymbol{\Lambda}_{11} & -\mathbf{S}_{12}\\ \mathbf{0} & \mathbf{0}\end{bmatrix}\begin{bmatrix}\dot{\boldsymbol{X}}_i\\ \dot{\boldsymbol{X}}_d\end{bmatrix} \\ &\quad = \begin{bmatrix}\mathbf{K}\mathbf{F}_i & \mathbf{K}\mathbf{F}\\ -\mathbf{S}_{12}^{\mathrm{T}}\mathbf{F}_i - \boldsymbol{\Lambda}_{22}\mathbf{F}^{\mathrm{T}} & -\mathbf{S}_{12}^{\mathrm{T}}\mathbf{F} - \boldsymbol{\Lambda}_{22}\mathbf{F}_d\end{bmatrix}\begin{bmatrix}\boldsymbol{X}_i\\ \boldsymbol{X}_d\end{bmatrix} \\ &\qquad + \begin{bmatrix}\mathbf{S}_{14} + \mathbf{S}_{13}\mathbf{H}\,\mathbf{S}_{34}\\ \mathbf{S}_{24}\end{bmatrix}\boldsymbol{U}\end{aligned} \tag{12}$$

where $\mathbf{H} = \mathbf{L}\left(\boldsymbol{\Lambda}_{33} - \mathbf{S}_{33}\mathbf{L}\right)^{-1}$ and $\mathbf{K} = \mathbf{S}_{11} + \mathbf{S}_{13}\mathbf{H}\,\mathbf{S}_{31}$.

To obtain equation (12), the following procedure is proposed.

A procedure for finding the state equations of a hybrid bond graph

1. Construct the diagonal matrix $\boldsymbol{\Lambda}$.
   (a) Consider each 1-port element in dynamic causality in turn and determine all paths of dynamic causality between these elements and the controlled junctions.
   (b) Use a truth table to construct the combination of states, and hence function of Boolean variables, that result in each causal change.
2. Construct the HJSM in the form of equation (3).
   (a) The HJSM relates system inputs to outputs. For elements in static causality, there will be one input and one output. For elements in dynamic causality, there are two inputs (effort and flow) and two outputs.
   (b) The HJSM is constructed by using ones and zeros to denote whether quantities are related or not.
   (c) Where a path between two elements crosses a TF or GY element, a variable or function other than one may appear in the HJSM.
   (d) Where a path between two elements crosses a controlled junction, a λ (or function of λ) is used to show that the relationship only occurs when the junction is ON (or OFF).
   (e) Where an element is in dynamic causality (shown by a dotted causal stroke in addition to the solid one), each variable will only be an input to the system in certain modes of operation. Referring to the truth table constructed in step 1, assign a function of λ, which denotes the modes in which the variable is an input.
   (f) Recall that the matrix should be skew-symmetric and sub-matrices $\mathbf{S_{22}}$, $\mathbf{S_{23}}$ and $\mathbf{S_{32}}$ should be zeros.
3. Derive the LTI implicit form.
   (a) Find matrices $\mathbf{L}$ and $\mathbf{F}$ from the (linear) relationships in the 1-port elements.
   (b) Take the sub-matrices of $\mathbf{S}$ and Λ from the JSM equation and insert them into the general LTI implicit form in equation (12).
   (c) Simplify this equation to give the implicit state equations plus some additional equations relating to the pseudo-states.

Properties of the space model

Properties of the model in one mode

Recall equation (12), which gives the model for all potential modes of operation. To assess a single mode of operation, the Boolean terms in Λ and the JSM $\mathbf{S}$ must be set to ones and zeros (denoting where each controlled junction is ON or OFF). There will be some redundancy in the equation, where some lines are zeros and can be deleted. This will give an equation of reduced order

$$\begin{bmatrix} \mathbf{I} & -\mathbf{S}_{12} \\ \mathbf{0} & \mathbf{0} \end{bmatrix} \begin{bmatrix} \dot{\boldsymbol{X}}_i \\ \dot{\boldsymbol{X}}_d \end{bmatrix} = \begin{bmatrix} (\mathbf{S}_{11}+\mathbf{S}_{13}\mathbf{H}\,\mathbf{S}_{31})\,\mathbf{F}_i & (\mathbf{S}_{11}+\mathbf{S}_{13}\mathbf{H}\,\mathbf{S}_{31})\,\mathbf{F} \\ -\mathbf{S}_{12}^{\mathrm{T}}\mathbf{F}_i-\mathbf{F}^{\mathrm{T}} & -\mathbf{S}_{12}^{\mathrm{T}}\mathbf{F}-\mathbf{F}_d \end{bmatrix} \begin{bmatrix} \boldsymbol{X}_i \\ \boldsymbol{X}_d \end{bmatrix} + \begin{bmatrix} \mathbf{S}_{14}+\mathbf{S}_{13}\mathbf{H}\,\mathbf{S}_{34} \\ \mathbf{S}_{24} \end{bmatrix} \boldsymbol{U} \tag{13}$$

where the matrices $\mathbf{S}_{ij}$ are evaluated for the parameters λ of the controlled junctions in the mode of operation and all null rows are removed.

For a reference mode where all storage elements are in integral causality, $\boldsymbol{\Lambda_{11}}$ is an identity matrix and $\mathbf{S_{12}}$ is a matrix of zeros. The second rows of $\boldsymbol{\Lambda}$ and $\mathbf{S}$ also become zero since this line would relate to elements in derivative causality. Equation (12) therefore becomes an ordinary state equation

$$\dot{\boldsymbol{X}}_i = [(\mathbf{S}_{11}+\mathbf{S}_{13}\mathbf{H}\,\mathbf{S}_{31})\,\mathbf{F}_i]\,\boldsymbol{X}_i + [\mathbf{S}_{14}+\mathbf{S}_{13}\mathbf{H}\,\mathbf{S}_{34}]\boldsymbol{U} \tag{14}$$

The resulting state equation for one mode can be manipulated and analysed for the properties of that mode as already described extensively in the literature. For example, it can be put into Smith or Kronecker canonical forms to allow inspection of the dynamics.

Properties of the general model

Equation (12) is comparable to the upper rows of the implicit state equation derived by Buisson et al.[20] using switched sources. In their model, the additional lower rows relate to the switch states, whereas here the switching manifests in the sub-matrices of $\mathbf{S}$.

The effect of commutation on the system dynamics can be clearly seen by manipulating the system equations into alternative canonical forms. This can be done for the system in one mode of operation or for the full model in which case the effects of commutation on the system dynamics can be seen. It follows that structural properties (observability and controllability, asymptotic stability and dynamic properties such as gain and the number of zeros and poles) can be functions of structural switching.

Comparison with switching sources and non-ideal approach

The 'Introduction' section highlighted the fact that the bulk of work to date on hybrid bond graph structural analysis has been conducted using switching sources. This section compares equation generated from a switched bond graph as developed by Buisson et al.[20] with the one obtained in this article and also investigates how the ideal controlled junction can be modified to account for dissipative effect on commutation.

Implicit state equations

Hybrid models constructed using switching sources are built for an initial (reference) mode, and subsequent modes of operation are derived from it (as opposed to building a model for all modes and deriving the equations for a single mode after). The JSM and standard implicit state equation contain extra states ($\boldsymbol{T}_i$ and $\boldsymbol{T}_o$) relating to the input and output to the switch(es). These rows contain the constitutive relation for the switches in terms of a commutation matrix $\boldsymbol{\Lambda}$. Note that the indices of $\mathbf{S}$ are slightly different, because the JSM also has additional terms due to $\boldsymbol{T}_i$ and $\boldsymbol{T}_o$, and that $\boldsymbol{\Lambda}$ is a square diagonal matrix with terms that are 1 or 0 depending on whether a switch has commutated. Buisson et al.[20] note that this form is not suitable for simulation

$$\begin{bmatrix} \mathbf{I} & -\mathbf{S}_{12} & \mathbf{0} & \mathbf{0} \\ \mathbf{0} & \mathbf{0} & \mathbf{0} & \mathbf{0} \\ \mathbf{0} & \mathbf{S}_{24}^{\mathrm{T}} & \mathbf{0} & \mathbf{0} \\ \mathbf{0} & \mathbf{0} & \mathbf{0} & \mathbf{0} \end{bmatrix} \begin{bmatrix} \dot{\boldsymbol{X}}_i \\ \dot{\boldsymbol{X}}_d \\ \dot{\boldsymbol{T}}_i \\ \dot{\boldsymbol{T}}_o \end{bmatrix} = \begin{bmatrix} \mathbf{K}\mathbf{F}_i & \mathbf{K}\mathbf{F} & \mathbf{S}_{14}+\mathbf{S}_{13}\mathbf{H}\,\mathbf{S}_{24} & \mathbf{0} \\ -\mathbf{S}_{12}^{\mathrm{T}}\mathbf{F}_i-\mathbf{F}^{\mathrm{T}} & -\mathbf{S}_{12}^{\mathrm{T}}\mathbf{F}-\mathbf{F}_d & \mathbf{S}_{24} & \mathbf{0} \\ -(\mathbf{S}_{14}^{\mathrm{T}}-\mathbf{S}_{34}^{\mathrm{T}}\mathbf{H}\mathbf{S}_{13}^{\mathrm{T}}) & \mathbf{0} & \mathbf{S}_{14}-\mathbf{S}_{34}^{\mathrm{T}}\mathbf{H}\,\mathbf{S}_{34} & -\mathbf{I} \\ \mathbf{0} & \mathbf{0} & \mathbf{I}-\boldsymbol{\Lambda} & \boldsymbol{\Lambda} \end{bmatrix} \times \begin{bmatrix} \boldsymbol{X}_i \\ \boldsymbol{X}_d \\ \boldsymbol{T}_i \\ \boldsymbol{T}_o \end{bmatrix} + \begin{bmatrix} \mathbf{S}_{15}+\mathbf{S}_{13}\mathbf{H}\,\mathbf{S}_{35} \\ \mathbf{S}_{25} \\ \mathbf{S}_{45}-\mathbf{S}_{34}^{\mathrm{T}}\mathbf{H}\,\mathbf{S}_{35} \\ \mathbf{0} \end{bmatrix} \boldsymbol{U} \tag{15}$$

where $\mathbf{H} = \mathbf{L}(\mathbf{I}-\mathbf{S}_{33}\mathbf{L})^{-1}$ and $\mathbf{K} = \mathbf{S}_{11} + \mathbf{S}_{13}\mathbf{H}\,\mathbf{S}_{31}$.

This standard implicit form is compared with the model in equation (12), reproduced below, and which is derived in this article for a model using controlled junctions. The different indices of the sub-matrices reflect the smaller JSM, and Boolean variables occur throughout the equation in the $\mathbf{S}$ and $\boldsymbol{\Lambda}$ sub-matrices

$$\begin{bmatrix} \boldsymbol{\Lambda}_{11} & -\mathbf{S}_{12} \\ \mathbf{0} & \mathbf{0} \end{bmatrix} \begin{bmatrix} \dot{\boldsymbol{X}}_i \\ \dot{\boldsymbol{X}}_d \end{bmatrix} = \begin{bmatrix} \mathbf{K}\mathbf{F}_i & \mathbf{K}\mathbf{F} \\ -\mathbf{S}_{12}^{\mathrm{T}}\mathbf{F}_i-\boldsymbol{\Lambda}_{22}\mathbf{F}^{\mathrm{T}} & -\mathbf{S}_{12}^{\mathrm{T}}F-\boldsymbol{\Lambda}_{22}\mathbf{F}_d \end{bmatrix} \begin{bmatrix} \boldsymbol{X}_i \\ \boldsymbol{X}_d \end{bmatrix} + \begin{bmatrix} \mathbf{S}_{14}+\mathbf{S}_{13}\mathbf{H}\,\mathbf{S}_{34} \\ \mathbf{S}_{24} \end{bmatrix} \boldsymbol{U}$$

where $\mathbf{H} = \mathbf{L}(\boldsymbol{\Lambda}_{33}-\mathbf{S}_{33}\mathbf{L})^{-1}$ and $\mathbf{K} = \mathbf{S}_{11} + \mathbf{S}_{13}\mathbf{H}\,\mathbf{S}_{31}$.

By selecting a single mode, the terms of $\boldsymbol{\Lambda}$ are given finite values. Hence, equations for a single mode comparable to the standard equation (and suitable for simulation) can be obtained.

While the implicit state equation (15) proposed by Buisson et al.[20] is obtained using straightforward standard bond graph techniques, the model is derived and valid for a reference configuration only. Recovering the implicit form for any other configuration requires

complex matrix operations because of elements changing the causality and the dimension and components of key vectors $\boldsymbol{X}_i, \boldsymbol{X}_d, \ldots$ changing accordingly. In the approach proposed in this article, non-standard techniques are used to generate the unique implicit state equation (12) that encompasses all configurations. Once the model (12) is obtained, any configuration can easily be obtained by evaluating Boolean expressions for the associated combination of switches. Due to the fact that the method exploits the graphical properties of causal bond graphs combined with some symbolic operations, it is believed that the method can be conveniently implemented in existing software such as SYMBOLS[49] or transferred to an environment like EcosimPro.[50]

Ideal and non-ideal approaches

Both switching sources and controlled junctions are ideal approaches, that is, no energy is dissipated on commutation. This is in contrast to earlier work using non-ideal approaches, that is, switches modelled by modulated resistors (MR) or resistors associated with modulated transformers (MTF) (which gives a unique, causally static bond graph). Buisson et al.[20] discuss ideal and non-ideal modelling and show that the ideal approach is a limit case of the non-ideal approach.

In some cases, a system cannot be assumed to be ideal (e.g. a hydraulic valve that acts as an orifice when open) and dissipation needs to be modelled. Buisson et al.[20] propose a semi-ideal approach, where the switching source is modelled as a variable resistance, and the constitutive relationship for the switching variables includes a resistance term.

Controlled junctions can be easily made semi-ideal in a similar manner, by simply adding a resistance element so as to dissipate energy when the junction is 'ON'. An interesting feature of the hybrid bond graph presented in this article is that the non-ideal case is remarkably similar to the Boolean MTF and resistor representation (MTF-R) proposed by Dauphin-Tanguy and Rombaut[38] and used most recently in a causally static form by Borutzky (Figure 5).[39] A comparison of an example system is shown in Figure 2, which is typical of an electrical switch.

In both cases, the R-element imposes flow on the junction. When $\lambda = 0$ (i.e. the switch is OFF), the flow is zero and the effort associated with the resistance is disconnected from the system. When $\lambda = 1$ (i.e. the switch is ON), the flow is governed by the R-element as a function of effort. The dynamic causality associated with the controlled junction is limited to the R-element. The similarity holds for switching parts where effort commutates between zero and a finite quantity (shown in Figure 6), typical of mechanical and hydraulic switching devices.

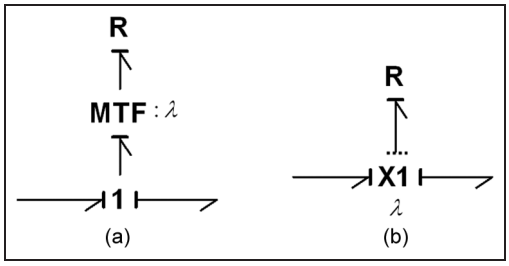

Figure 5. An example of causality assignment around a non-ideal (flow) switch: (a) the switch represented by a Boolean MTF and resistor and (b) the switch represented by a controlled junction and additional resistance.
MTF: modulated transformer.

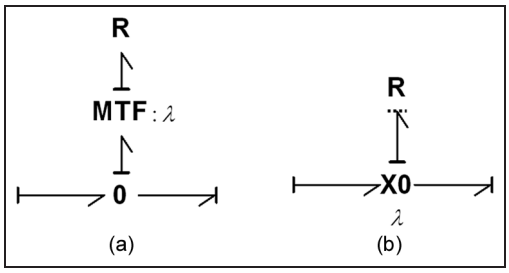

Figure 6. An example of causality assignment around a non-ideal (effort) switch: (a) the switch represented by a Boolean MTF and resistor and (b) the switch represented by a controlled junction and additional resistance.

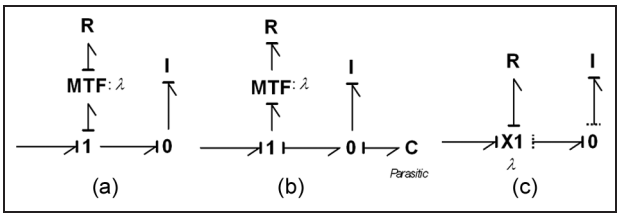

Figure 7. An example system with a non-ideal (flow) switch: (a) the switch represented by a Boolean MTF and resistor, (b) a parasitic element added to control causality and ensure that the MTF-R acts as a switch and (c) the switch represented by a controlled junction.

However, the similarity between the two techniques does not always hold true: there are cases where the R-element does not govern the flow on a 1-junction (or effort on a 0-junction). In these cases, the MTF-R representation would not act as a switch (because it would not be imposing a null quantity on the system: it would simply disconnect the R-element): parasitic elements may need to be added to the model to manipulate the causal assignment, as shown in Figure 7. This would be the case for systems where the non-ideal switch is modelled using a modulated resistance too. The controlled junction, however, works regardless of the causal assignment on the incident bonds. Note that a

kinematic constraint exists between the controlled junction and the I-element when the switch is 'off': the analyst may now make an informed decision whether to revise the modelling assumptions, break this constraint using parasitic elements or allow it to remain.

Example

Hybrid bond graph of a power converter

A boost converter is shown in Figure 8, as an example incorporating both electrical switches and a mechanical clutch. Buisson et al.[20] use this example to demonstrate the use of switching sources, as do Edström et al.[11] on a simplified version. Here, controlled junctions will be used. The bond graph of the power converter is shown in Figure 9. Note that some resistance elements have been added (R_1 and R_2) to model losses in the circuit and friction in the moving parts. The full bond graph, incorporating the ground, is shown for completeness, and then systematically simplified by removing bonds to the ground (which is 0 V) where appropriate. The ground still needs to be represented and attached to switch 2; it is worth noting that this source and controlled junction arrangement are remarkably similar to the switching source in principle.

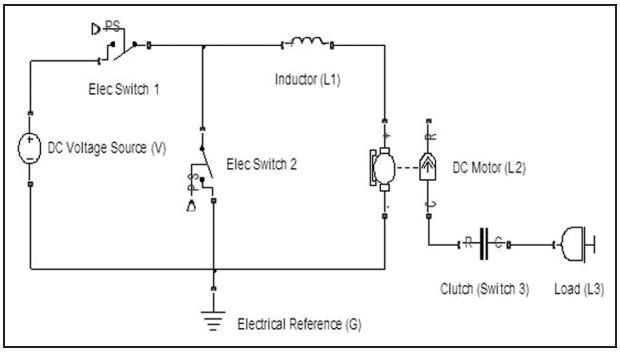

Figure 8. Schematic diagram of a boost converter supplying a DC motor with load.
DC: direct current.

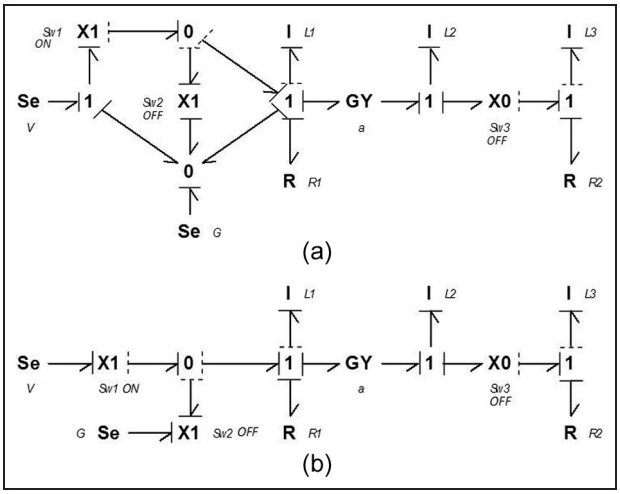

Figure 9. Hybrid bond graph model of the boost converter: (a) complete model and (b) simplified model.

Modes of operation and allowed configurations

In order to construct the JSM, the modes of operation and any consequential dynamic causality must be identified. This gives the functions of λ used in the JSM and state equations. These are in turn used to construct a matrix $\mathbf{\Lambda}$, which multiplies the equation by zeros and ones to ensure that state variables disappear from the model when they are not part of a mode of operation.

The solid causal strokes in Figure 9 show the reference configuration, which is the configuration in which the most storage elements are in integral causality. This is given by switch 1 being ON and switches 2 and 3 being OFF. Note that it would also be given if switch 1 was OFF and switch 2 was ON; in this case, a reference mode can be selected arbitrarily. Dashed causal lines show the alternative causality assignment where causality is dynamic (i.e. it changes with mode of operation). Note that controlled junctions become a source of zero flow/effort when they are 'OFF', which means that they do not take any other flow/effort inputs in that mode of operation. The model inherently includes all possible modes of operation. This eases the construction of the JSM, and the user does not need to produce a bond graph or derive equations for each mode. 'Paths' of dynamic causality can be traced, showing the effect of switches on other elements (as shown in Table 4). It can

Table 4. Effects of switches on causality of 1-port elements.

Switch	Dynamic causal path to storage element?	Dynamic causal path to resistor element?
Switch 1	L_1	–
Switch 2	L_1	–
Switch 3	L_3	–

Table 5. Truth table of the effect of switches on dynamic causal elements.

Switch 1	Switch 2	Switch 3	Causality on L_1	Causality on L_3
0	0	–	Derivative	–
0	1	–	Integral	–
1	0	–	Integral	–
1	1	–	Causal conflict	–
–	–	0	–	Integral
–	–	1	–	Derivative

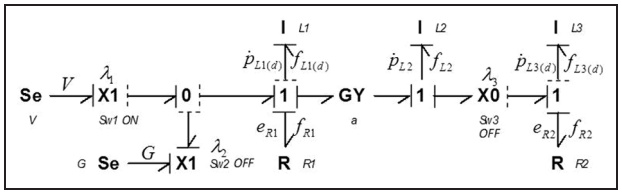

Figure 10. Hybrid bond graph model of the boost converter with notation.

be seen that switches 1 and 2 both affect the causal assignment of L_1, while switch 3 solely governs the assignment of L_3. In order to derive a switching rule for inclusion in the JSM (and, subsequently, the state space matrices), a truth table can be used. Looking at Table 5, it can be seen that L_3 is in integral causality when switch 3 is 'OFF'. The state variable must therefore be 'active' when switch 3 is 'OFF': this can be achieved by multiplying the relevant row of the JSM by a Boolean $\bar{\lambda}_3$ (equal to 1 when switch 3 is not 'on', and otherwise equal to 0). The pseudo-state variable is likewise activated when the switch is 'ON' by multiplying the relevant row of the JSM by the Boolean λ_3 (equal to 1 when switch 3 is 'ON').

Looking at Table 5, a slightly more complex Boolean expression must be defined. L_1 is in integral causality when switch 1 *or* switch 2 is 'ON'. The element is in derivative causality when both switches are 'OFF'. The case where both are 'ON' is a forbidden mode since the voltage source is short-circuited, and this is reflected by a causal conflict. The state variable can therefore be activated using a Boolean factor of $\lambda_1 \oplus \lambda_2$ where the symbol '$\oplus$' denotes an 'exclusive or' (XOR) operation. The pseudo-state variable is activated when this is not true, that is, $\overline{\lambda_1 \oplus \lambda_2}$.

Deriving the junction structure and implicit state equations

The JSM (given below) is constructed for a regular system, but includes further Booleans where an input/output depends on the state of a switch. The subscript '*d*' denotes derivative causality (Figure 10).

$$\Lambda \begin{bmatrix} \dot{p}_{L1} \\ \dot{p}_{L2} \\ \dot{p}_{L3} \\ f_{L1d} \\ f_{L3d} \\ f_{R1} \\ f_{R2} \end{bmatrix} = \begin{bmatrix} 0 & -a(\lambda_1 \oplus \lambda_2) & 0 & 0 & 0 \\ a(\lambda_1 \oplus \lambda_2) & 0 & 0 & 0 & -\lambda_3 \\ 0 & 0 & 0 & 0 & 0 \\ 0 & 0 & 0 & 0 & 0 \\ 0 & \lambda_3 & 0 & 0 & 0 \\ (\lambda_1 \oplus \lambda_2) & 0 & 0 & 0 & 0 \\ 0 & \lambda_3 & \bar{\lambda}_3 & 0 & 0 \end{bmatrix} \begin{bmatrix} -(\lambda_1 \oplus \lambda_2) & 0 & \lambda_1 & \lambda_2 \\ 0 & -\lambda_3 & 0 & 0 \\ 0 & -\bar{\lambda}_3 & 0 & 0 \\ 0 & 0 & 0 & 0 \\ 0 & 0 & 0 & 0 \\ 0 & 0 & 0 & 0 \\ 0 & 0 & 0 & 0 \end{bmatrix} \times \begin{bmatrix} f_{L1} \\ f_{L2} \\ f_{L3} \\ \dot{p}_{L1d} \\ \dot{p}_{L3d} \\ e_{R1} \\ e_{R2} \\ V \\ G \end{bmatrix} \tag{16}$$

where

$$\mathbf{\Lambda} = diag\left[(\lambda_1 \oplus \lambda_2) \quad 1 \quad \bar{\lambda}_3 \quad (\overline{\lambda_1 \oplus \lambda_2}) \quad \lambda_3 \quad 1 \quad 1\right] \tag{17}$$

Remember that controlled junctions are thought of as null sources when they are 'OFF'. The input flows and efforts representing the switches in the OFF position could be explicitly shown as inputs, but since these are inherently zero, it is sufficient to imply them by sending terms in the JSM to zero.

The state space matrices for this system seem a little complicated since there is a causal path between L_2 and L_3 (in derivative causality) when the clutch is engaged. This can be seen from the coefficient in sub-matrices $\mathbf{S_{21}}$ and $\mathbf{S_{12}}$ of the JSM. If the classical state equations were to be found, there may be a motivation here for adding a parasitic element to break the causal path. Instead, the use of pseudo-states for those elements in derivative causality handles the loop. The constitutive law of the R-field is

$$\begin{aligned} D_{in} &= \mathbf{L}\, D_{out} \\ \begin{bmatrix} f_{R1} \\ f_{R2} \end{bmatrix} &= \begin{bmatrix} R_1^{-1} & 0 \\ 0 & R_2^{-1} \end{bmatrix} \begin{bmatrix} e_{R1} \\ e_{R2} \end{bmatrix} \end{aligned} \tag{18}$$

A matrix $\mathbf{H}$ can be defined as $\mathbf{H} = \begin{bmatrix} R_1 & 0 \\ 0 & R_2 \end{bmatrix}$. The constitutive law for the storage elements is as follows

$$\begin{bmatrix} Z_i \\ Z_d \end{bmatrix} = \begin{bmatrix} \mathbf{F}_i & \mathbf{F} \\ \mathbf{F}^{\mathrm{T}} & \mathbf{F}_d \end{bmatrix} \begin{bmatrix} X_i \\ X_d \end{bmatrix} \tag{19}$$

where $\mathbf{F}_i = \begin{bmatrix} L_1^{-1} & 0 & 0 \\ 0 & L_2^{-1} & 0 \\ 0 & 0 & L_3^{-1} \end{bmatrix}$, $\mathbf{F}_d = \begin{bmatrix} {L_1}^{-1} & 0 \\ 0 & {L_3}^{-1} \end{bmatrix}$ and $\mathbf{F} = \begin{bmatrix} 0 & 0 \\ 0 & 0 \\ 0 & 0 \end{bmatrix}$.

Using equation (2), the state space equations for the power converter example are therefore given as follows

For the reference configuration ($\lambda_1 = 1$, $\lambda_2 = 0$ and $\lambda_3 = 0$), this gives

$$\begin{bmatrix} (\lambda_1 \oplus \lambda_2) & 0 & 0 & 0 & 0 \\ 0 & 1 & 0 & 0 & \lambda_3 \\ 0 & 0 & \bar{\lambda}_3 & 0 & 0 \\ 0 & 0 & 0 & 0 & 0 \\ 0 & 0 & 0 & 0 & 0 \end{bmatrix} \begin{bmatrix} \dot{p}_{L1} \\ \dot{p}_{L2} \\ \dot{p}_{L3} \\ \dot{p}_{L1d} \\ \dot{p}_{L3d} \end{bmatrix} = \begin{bmatrix} \frac{-(\lambda_1 \oplus \lambda_2)}{L_1 R_1} & \frac{-a(\lambda_1 \oplus \lambda_2)}{L_2} & 0 & 0 & 0 \\ \frac{a(\lambda_1 \oplus \lambda_2)}{L_1} & \frac{-\lambda_3}{L_2 R_2} & 0 & 0 & 0 \\ 0 & 0 & \frac{-\bar{\lambda}_3}{L_3 R_2} & 0 & 0 \\ 0 & 0 & 0 & \frac{(\lambda_1 \oplus \lambda_2)}{L_1} & 0 \\ 0 & \frac{\lambda_3}{L_2} & 0 & 0 & -\frac{\lambda_3}{L_3} \end{bmatrix} \begin{bmatrix} p_{L1} \\ p_{L2} \\ p_{L3} \\ p_{L1d} \\ p_{L3d} \end{bmatrix} + \begin{bmatrix} \lambda_1 & \lambda_2 \\ 0 & 0 \\ 0 & 0 \\ 0 & 0 \\ 0 & 0 \end{bmatrix} \begin{bmatrix} V \\ G \end{bmatrix} \quad (20)$$

$$\begin{bmatrix} 1 & 0 & 0 & 0 & 0 \\ 0 & 1 & 0 & 0 & 0 \\ 0 & 0 & 1 & 0 & 0 \\ 0 & 0 & 0 & 0 & 0 \\ 0 & 0 & 0 & 0 & 0 \end{bmatrix} \begin{bmatrix} \dot{p}_{L1} \\ \dot{p}_{L2} \\ \dot{p}_{L3} \\ \dot{p}_{L1d} \\ \dot{p}_{L3d} \end{bmatrix}$$

$$= \begin{bmatrix} \frac{-1}{L_1 R_1} & \frac{-a}{L_2} & 0 & 0 & 0 \\ \frac{a}{L_1} & 0 & 0 & 0 & 0 \\ 0 & 0 & \frac{-1}{L_3 R_2} & 0 & 0 \\ 0 & 0 & 0 & 0 & 0 \\ 0 & 0 & 0 & 0 & 0 \end{bmatrix} \begin{bmatrix} p_{L1} \\ p_{L2} \\ p_{L3} \\ p_{L1d} \\ p_{L3d} \end{bmatrix} \quad (21)$$

$$+ \begin{bmatrix} 1 & 0 \\ 0 & 0 \\ 0 & 0 \\ 0 & 0 \\ 0 & 0 \end{bmatrix} \begin{bmatrix} V \\ G \end{bmatrix}$$

Giving the equations

$$\begin{aligned} \dot{p}_{L1} &= \frac{-1}{L_1 R_1} p_{L1} - \frac{a}{L_2} p_{L2} + V \\ \dot{p}_{L2} &= \frac{a}{L_1} p_{L1} \\ \dot{p}_{L3} &= \frac{-1}{L_3 R_2} p_{L3} \\ 0 &= 0 \\ 0 &= 0 \end{aligned} \quad (22)$$

There are state equations for each of the three storage elements in integral causality, as expected. With the clutch disengaged, the load L_3 is clearly disconnected from the rest of the system. For the case where most elements are in derivative causality ($\lambda_1 = 0$, $\lambda_2 = 0$ and $\lambda_3 = 1$)

$$\begin{bmatrix} 0 & 0 & 0 & 0 & 0 \\ 0 & 1 & 0 & 0 & 1 \\ 0 & 0 & 0 & 0 & 0 \\ 0 & 0 & 0 & 0 & 0 \\ 0 & 0 & 0 & 0 & 0 \end{bmatrix} \begin{bmatrix} \dot{p}_{L1} \\ \dot{p}_{L2} \\ \dot{p}_{L3} \\ \dot{p}_{L1d} \\ \dot{p}_{L3d} \end{bmatrix}$$

$$= \begin{bmatrix} 0 & 0 & 0 & 0 & 0 \\ 0 & \frac{-1}{L_2 R_2} & 0 & 0 & 0 \\ 0 & 0 & 0 & 0 & 0 \\ 0 & 0 & 0 & L_1^{-1} & 0 \\ 0 & L_2^{-1} & 0 & 0 & -L_3^{-1} \end{bmatrix} \begin{bmatrix} p_{L1} \\ p_{L2} \\ p_{L3} \\ p_{L1d} \\ p_{L3d} \end{bmatrix} + \begin{bmatrix} 0 & 0 \\ 0 & 0 \\ 0 & 0 \\ 0 & 0 \\ 0 & 0 \end{bmatrix} \begin{bmatrix} V \\ G \end{bmatrix} \quad (23)$$

Giving the equations

$$\begin{cases} 0 = 0 \\ \dot{p}_{L2} + \dot{p}_{L3d} = \frac{-1}{L_2 R_2} p_{L2} \\ 0 = 0 \\ 0 = \frac{1}{L_1} p_{L1d} \\ 0 = \frac{1}{L_2} p_{L2} - \frac{1}{L_3} p_{L3d} \end{cases} \quad (24)$$

With both electrical switches 'OFF' and the clutch engaged, the inertia of the direct current (DC) motor exerts no torque on the system and the load is not free to rotate. This is consistent with what would be expected.

An interesting case occurs in the mode where both switches 1 and 2 are 'ON'. This is a 'forbidden' mode, which short-circuits the voltage source and sets up a causal conflict in the bond graph. The equations are given as follows (assuming clutch is disengaged)

$$\begin{bmatrix} 0 & 0 & 0 & 0 & 0 \\ 0 & 1 & 0 & 0 & 0 \\ 0 & 0 & 1 & 0 & 0 \\ 0 & 0 & 0 & 0 & 0 \\ 0 & 0 & 0 & 0 & 0 \end{bmatrix} \begin{bmatrix} \dot{p}_{L1} \\ \dot{p}_{L2} \\ \dot{p}_{L3} \\ \dot{p}_{L1d} \\ \dot{p}_{L3d} \end{bmatrix} = \begin{bmatrix} 0 & 0 & 0 & 0 & 0 \\ 0 & 0 & 0 & 0 & 0 \\ 0 & 0 & \frac{-1}{L_3 R_2} & 0 & 0 \\ 0 & 0 & 0 & L_1^{-1} & 0 \\ 0 & 0 & 0 & 0 & 0 \end{bmatrix} \begin{bmatrix} p_{L1} \\ p_{L2} \\ p_{L3} \\ p_{L1d} \\ p_{L3d} \end{bmatrix} + \begin{bmatrix} 1 & 1 \\ 0 & 0 \\ 0 & 0 \\ 0 & 0 \\ 0 & 0 \end{bmatrix} \begin{bmatrix} V \\ G \end{bmatrix} \tag{25}$$

The first two lines give $V = -G$ and $\dot{p}_{L2} = 0$, that is, the input voltage is a function of the ground, and the mechanical load L_2 is not powered by the electrical circuit. This clearly reflects the short circuit.

Discontinuities on variables at commutation

Consider the case where the system is in the reference mode, and then the clutch (switch 3) engages. Recalling the reference configuration

$$\begin{bmatrix} 1 & 0 & 0 & 0 & 0 \\ 0 & 1 & 0 & 0 & 0 \\ 0 & 0 & 1 & 0 & 0 \\ 0 & 0 & 0 & 0 & 0 \\ 0 & 0 & 0 & 0 & 0 \end{bmatrix} \begin{bmatrix} \dot{p}_{L1} \\ \dot{p}_{L2} \\ \dot{p}_{L3} \\ \dot{p}_{L1d} \\ \dot{p}_{L3d} \end{bmatrix} = \begin{bmatrix} \frac{-1}{L_1 R_1} & -\frac{a}{L_2} & 0 & 0 & 0 \\ \frac{a}{L_1} & 0 & 0 & 0 & 0 \\ 0 & 0 & \frac{-1}{L_3 R_2} & 0 & 0 \\ 0 & 0 & 0 & 0 & 0 \\ 0 & 0 & 0 & 0 & 0 \end{bmatrix} \begin{bmatrix} p_{L1} \\ p_{L2} \\ p_{L3} \\ p_{L1d} \\ p_{L3d} \end{bmatrix} + \begin{bmatrix} 1 & 0 \\ 0 & 0 \\ 0 & 0 \\ 0 & 0 \\ 0 & 0 \end{bmatrix} \begin{bmatrix} V \\ G \end{bmatrix} \tag{26}$$

After the clutch connects

$$\begin{bmatrix} 1 & 0 & 0 & 0 & 0 \\ 0 & 1 & 0 & 0 & 1 \\ 0 & 0 & 0 & 0 & 0 \\ 0 & 0 & 0 & 0 & 0 \\ 0 & 0 & 0 & 0 & 0 \end{bmatrix} \begin{bmatrix} \dot{p}_{L1} \\ \dot{p}_{L2} \\ \dot{p}_{L3} \\ \dot{p}_{L1d} \\ \dot{p}_{L3d} \end{bmatrix} = \begin{bmatrix} \frac{-1}{L_1 R_1} & \frac{-a}{L_2} & 0 & 0 & 0 \\ \frac{a}{L_1} & \frac{-1}{L_2 R_2} & 0 & 0 & 0 \\ 0 & 0 & 0 & 0 & 0 \\ 0 & 0 & 0 & 0 & 0 \\ 0 & L_2^{-1} & 0 & 0 & -L_3^{-1} \end{bmatrix} \begin{bmatrix} p_{L1} \\ p_{L2} \\ p_{L3} \\ p_{L1d} \\ p_{L3d} \end{bmatrix} + \begin{bmatrix} 1 & 0 \\ 0 & 0 \\ 0 & 0 \\ 0 & 0 \\ 0 & 0 \end{bmatrix} \begin{bmatrix} V \\ G \end{bmatrix} \tag{27}$$

The equations are as follows:

Reference configuration

$$\begin{cases} \dot{p}_{L1} = \dfrac{-1}{L_1 R_1} p_{L1} - \dfrac{a}{L_2} p_{L2} + V \\ \dot{p}_{L2} = -\dfrac{a}{L_1} p_{L1} \\ \dot{p}_{L3} = \dfrac{-1}{L_3 R_2} p_{L3} \end{cases} \tag{28}$$

Clutch engaged

$$\begin{cases} \dot{p}_{L1} = \dfrac{-1}{L_1 R_1} p_{L1} - \dfrac{a}{L_2} p_{L2} + V \\ \dot{p}_{L2} + \dot{p}_{L3d} = -\dfrac{a}{L_1} p_{L1} - \dfrac{1}{L_2 R_2} p_{L2} \\ 0 = \dfrac{1}{L_2} p_{L2} - \dfrac{1}{L_3} p_{L3d} \end{cases} \tag{29}$$

The system changes from having three differential state equations to having two differential equations and an associated algebraic relationship. The equation for $\dot{p}_{L1}$ remains unchanged with commutation. The equation for $\dot{p}_{L2}$ becomes a function of p_{L2} and pseudo-state $\dot{p}_{L3d}$ in addition to p_{L1}, and the algebraic relation can be rearranged to give p_{L3d} in terms of p_{L2}. If the clutch commutes back from engaged to disengaged, the state of L_3 just after commutation is equal to the state just before, that is, $p_{L3d} = p_{L3}$ and $\dot{p}_{L3d} = \dot{p}_{L3}$ and there is no need to reinitialise the state.

In this model, any slippage occurring between fully engaged and fully disengaged would be modelled by resistance element R_2. Some authors would define slippage as an extra mode of operation. Here, the controlled junction purely represents whether contact has been made or not. Any additional non-linear dissipation can be modelled using a resistance element, which could itself be abstracted to discrete modes of operation. This is an example of parametric switching and will be addressed in the further work.

Conclusions

In this article, the controlled junction is selected to model 'structural discontinuities' (i.e. physical switching elements that change the power flow and structure of the model). It clearly and intuitively shows the effect of commutation in the bond graph and can be represented by a Boolean parameter in the JSM. Unlike other methods, there are no additional inputs to the system.

The general hybrid bond graph is presented as a general bond graph with a modified junction structure. The HJSM **S** is a function of a structural switching Boolean parameter λ as well as 0 and 1 (and coefficients relating to any transformers or gyrators). This Boolean parameter corresponds to the state of a controlled junction or combination of controlled junctions.

Dynamic causality is an inherent feature of this general hybrid bond graph and is allowed so as to prevent

any additional complexity or stiff dynamics and maximise insight into the model. A method for representing dynamic causality on a bond graph (using dashed causal strokes) is proposed. Equation generation and structural analysis techniques are extended to apply to the general hybrid bond graph. A single implicit equation describing all possible modes of operation is generated. The Boolean factors in the junction structure carry through into the state matrices. All modes of operation can be obtained directly from this equation, as opposed to deriving modes in relation to a reference. Where dynamic causality affects a 1-port element, two lines are defined in the JSM and are associated with a Boolean factor to (de)activate the line according to the state of the relevant controlled junctions. In deriving the implicit state equations, this gives rise to the use of pseudo-state variables to describe storage elements in dynamic causality.

This technique has been demonstrated on the case study of a power converter. Equations can be derived for each mode, including the short-circuit case. Possible further work is to consider non-linear models and to formalise the use of parametric discontinuities (e.g. piecewise continuous functions), to generate the general form of the implicit state equations. Also, automation of equation generation and simulation, and possible implementation of the proposed method in existing software, will be the theme of further research.

Funding

This study was supported by the EPSRC and Airbus Operations Ltd via a CASE award.

References

1. Thoma JU. *Introduction to bond graphs and their applications*. 1st ed. Oxford: Pergamon Press, 1975.
2. Dransfield P. (ed.) Hydraulic control systems – design and analysis of their dynamics. In: Balakrishnan AV and Thoma M (eds) *Lecture notes in control and information sciences*, vol. 33. 1st ed. Berlin: Springer-Verlag, 1981.
3. Castelain A, Ducreux J-P, Dauphin-Tanguy G, et al. *Modelling and analysis of power electronic networks by bond graph*. MSc Thesis, IMACS (TCI '90), France, 1990.
4. Asher, GM. The robust modelling of variable topology circuits using bond graphs, *International conference on bond graph modeling, January 17–20, 1993, La Jolla, California: ICBGM '93: Proceedings of the 1993 Western simulation multiconference*. La Jolla, California, 17–20 January 1993, pp.126–131. San Diego: Society for Computer Simulation International.
5. Strömberg JE, Top J and Soderman U. Variable causality in bond graphs caused by discrete effects. In: *International conference on bond graph modeling, January 17–20, 1993, La Jolla, California: ICBGM '93 : Proceedings of the 1993 Western simulation multiconference*. La Jolla, California, 17–20 January 1993, pp.115–119. San Diego: Society for Computer Simulation International.
6. Mosterman PJ and Biswas, G. Modeling discontinuous behavior with hybrid bond graphs. In: *Proceedings of the 9th international workshop on qualitative reasoning about physical systems*, Amsterdam, The Netherlands, 16–19 May 1995, pp.139–147. Amsterdam: University of Amsterdam.
7. Gawthrop PJ. *Hybrid bond graphs using switched I and C components*. *Technical Report CSC-97005*, Glasgow, UK: Faculty of Engineering, University of Glasgow, 1997.
8. Borutzky W. Discontinuities in a bond graph framework. *J Frankl I* 1995; 332B(2): 141–154.
9. Kofman E and Junco S. Quantized bond graphs: an approach for discrete event simulation of physical systems. In: *Proceedings of the 2001 international conference on bond graph modeling and simulation (ICBGM '01)*, Phoenix, Arizona, 7–11 January 2001, pp.369–374. San Diego: Society for Computer Simulation International.
10. Zimmer D and Cellier FE. Impulse-bond graphs. In: *Proceedings of the 2007 International conference on bond graph modeling: ICBGM 2007*, San Diego, California, 14–17 January 2007, pp.3–11. San Diego: Society for Computer Simulation International.
11. Edström K, Strömberg JE, Soderman U, et al. Modelling and simulation of a switched power converter. *Simul Series* 1997; 29(1): 195–200.
12. Edstrom K, Stromberg JE and Top J. Aspects on simulation of switched bond graphs. In: *Proceedings of the 35th IEEE conference on decision and control*, Kobe, Japan, 11–13 December 1996, pp.2642–2647. New Jersey: IEEE.
13. Mosterman PJ. An overview of hybrid simulation phenomena and their support by simulation packages. In: Vaandrager FW and van Schuppen JH (eds) *Hybrid systems: computation and control*. Berlin: Springer. pp.165–177.
14. Mosterman PJ and Biswas G. Formal specifications for hybrid dynamical systems. In: *Proceedings of the Fifteenth international joint conference on artificial intelligence, IJCAI-97*, Nagoya, Japan, 23–29 August 1997, pp. 568–573. San Francisco: Kaufmann.
15. Mosterman PJ and Biswas G. A theory of discontinuities in physical system models. *J Frankl Inst* 1997; 335B(3): 401–439.
16. Mosterman PJ and Biswas G. A comprehensive methodology for building hybrid models of physical systems. *Artif Intell* 2000; 121(1–2): 171–209.
17. Mosterman PJ, Broenink JF and Biswas G. Model semantics and simulation of time scale abstractions in collision models. In: *3rd International congress of the federation of EUROpean SIMulation Societies*, Helsinki, Finland, 14–17 April 1998, pp.230–237. Amsterdam: Elsevier Science.
18. Mosterman PJ, Zhao F, Biswas G, et al. An ontology for transitions in physical dynamic systems. In: *Proceedings: Fifteenth national conference on artificial intelligence (AAAI-98)*, Menlo Park, California, 26–30 July 1998, pp.219–224. AAAI Press.
19. Edström K. *Switched bond graphs: simulation and analysis*. PhD Thesis No. 586, Linköpings Universitet, Sweden, 1999.
20. Buisson J, Cormerais H and Richard PY. Analysis of the bond graph model of hybrid physical systems with ideal switches. *Proc IMechE, Part I: J Systems and Control Engineering* 2002; 216(1): 47–63.
21. Dauphin-Tanguy G and Sueur C. Bond graph for modelling, analysis, control design, fault diagnosis. www.fceia.

unr.edu.ar/~kofman/seminario/Argentine-nov02.ppt (2002, accessed 2010).
22. Djeziri MA, Merzouki R, Bouamama BO, et al. Fault detection of backlash phenomenon in mechatronic system with parameter uncertainties using bond graph approach. In: *Proceedings 2006 international conference on mechatronics and automation, IEEE ICMA*, Luoyang, Henan, China, 25–28 June 2006, pp.600–605. New Jersey: IEEE.
23. Rahmani A and Dauphin-Tanguy G. Structural analysis of switching systems modelled by bond graph. *Math Comp Model Dyn* 2006; 12(2–3): 235–247.
24. Djeziri MA, Merzouki R, Bouarnarria BO, et al. Robust fault diagnosis by using bond graph approach. *IEEE-ASME T Mech* 2007; 12(6): 599–611.
25. Richard PY, Morarescu M and Buisson J. Bond graph modelling of hard nonlinearities in mechanics: a hybrid approach. *Nonlinear Anal Hybrid Syst* 2008; 2: 922–951.
26. Borutzky W. *Bond graph methodology: development and analysis of multi-disciplinary dynamic system models*. 1st ed. London: Springer-Verlag London Ltd, 2010.
27. Breedveld PC. An alternative model for static and dynamic friction in dynamic system simulation. In: *1st IFAC conference on mechatronic systems*, Darmstadt, Germany, 18–20 September 2000, pp.717–722. Düsseldorf, Germany: International Federation of Automatic Control, VDI/VDE Geselleschaft.
28. Breedveld PC. Modelling & simulation of bouncing objects: Newton's cradle revisited. In: *Proceedings mechatronics 2002: 8th mechatronics forum international conference*, University of Twente, 24–26 June 2002, pp.810–819. UK: Mechatronics Forum.
29. Daigle MJ, Koutsoukos XD and Biswas G. A qualitative event-based approach to continuous systems diagnosis. *IEEE T Contr Syst T* 2009; 17(4): 780–793.
30. Lattmann Z. *A multi-domain functional dependency modeling tool based on extended hybrid bond graphs*. MSc Thesis, Department of Electrical Engineering, Vanderbilt University, Nashville, TN, 2010, p.40.
31. Narasimhan S. *Model-based diagnosis of hybrid systems*. Doctor Dissertation, Department of Computer Science, Vanderbilt University, Nashville, TN, 2002.
32. Podgursky B, Biswas G and Koutsoukos XD. Efficient tracking of behavior in complex hybrid systems via hybrid bond graphs. In: *Annual conference of the prognostics and health management society (PHM 2010)*, Portland, Oregon, 10–14 October 2010. Ft. Belvoir: Defense Technical Information Center.
33. Roychoudhury I. Efficient simulation of hybrid systems: a hybrid bond graph approach. *Simulation* 2011; 87(6): 467–498.
34. Low C. Monitoring ability analysis and qualitative fault diagnosis using hybrid bond graph. *IFAC Proc Vol (IFAC-PapersOnline)* 2008; 17(1). Available from www.ifac-papersonline.net/ (accessed 2011).
35. Low CB, Wang D, Arogeti S, et al. Causality assignment and model approximation for hybrid bond graph: fault diagnosis perspectives. *IEEE T Autom Sci Eng* 2010; 7(Compendex): 570–580.
36. Low CB, Wang D, Arogeti SA, et al. Fault parameter estimation for hybrid systems using hybrid bond graph. In: *2009 IEEE control applications (CCA) & intelligent control (ISIC)*, St. Petersburg, Russia, 8–10 July 2009, pp.1338–1343. New Jersey: IEEE.
37. Umarikar AC and Umanand L. Modelling of switching systems in bond graphs using the concept of switched power junctions. *J Frankl Inst* 2005; 342: 131–147.
38. Dauphin-Tanguy G and Rombaut C. Why a unique causality in the elementary commutation cell bond graph model of a power electronics converter. In: *Conference proceedings, international conference on systems, man and cybernetics, 1993. 'Systems engineering in the service of humans'*, Le Touquet, France, 17–20 October 1993, pp.257–263. New York: IEEE.
39. Borutzky W. Bond-graph-based fault detection and isolation for hybrid system models. *Proc IMechE, Part I: J Systems and Control Engineering* 2012; 226(6): 742–760.
40. Rosenberg RC. Exploiting bond graph causality in physical system models. *J Dyn Syst: T ASME* 1987; 109(4): 378–383.
41. Sueur C and Dauphin-Tanguy G. Structural controllability/observability of linear systems represented by bond graphs. *J Frankl Inst* 1989; 326(6): 869–883.
42. Ort JR and Martens HR. Properties of bond graph junction structure matrices. *J Dyn Syst: T ASME* 1973; 95(4): 362–367.
43. Perelson AS. Bond graph junction structures. *J Dyn Syst: T ASME* 1975; 97(2): 189–195.
44. Bidard C, Favret F, Goldztejn S, et al. Bond graph and variable causality. In: *Conference proceedings, international conference on systems, man and cybernetics, 1993. 'Systems engineering in the service of humans'*, Le Touquet, France, 17–20 October 1993, pp.270–275. New York: IEEE.
45. Cellier FE, Otter M and Elmqvist H. Bond graph modeling of variable structure systems. *Simul Series* 1994; 27(1): 49–55.
46. Buisson J. Analysis and characterization of hybrid systems with bond-graphs. In: *Conference proceedings, international conference on systems, man and cybernetics, 1993. 'Systems engineering in the service of humans'*, Le Touquet, France, 17–20 October 1993, pp.264–269. New York: IEEE.
47. Karnopp DC, Margolis DL and Rosenberg RC. *System dynamics modeling and simulation of mechatronic systems*. 4th ed. Hoboken, New Jersey: John Wiley & Sons, Inc., 2006.
48. Sueur C and Dauphin-Tanguy G. Bond graph approach to multi-time scale systems analysis. *J Frankl I* 1991; 328(5–6): 1005–1026.
49. Hightech Consultants. http://www.htcinfo.com/ (accessed 22 August 2012).
50. EcosimPro Modelling and Simulation Software. http://www.ecosimpro.com/index.php (accessed 22 August 2012).

Appendix 1

Notation

A	**A** matrix in the standard linear time-invariant state space equation
B	**B** matrix in the standard linear time-invariant state space equation
D	vector of input/output variables to the resistance field
e	generalised effort variable on a bond
f	generalised flow variable on a bond

F	diagonal matrix of the linear coefficients for storage elements (relating the states to their complements)
G	ground
L	diagonal matrix of the linear coefficients for resistance elements (relating the outputs to inputs)
L	linear coefficient for a single inertia (I-element)
p	momentum
q	displacement
R	linear coefficient for a single resistance (R-element)
S	junction structure matrix
$\boldsymbol{T}$	vector of input/output variables to switched sources
$\boldsymbol{U}$	input vector to the system
$\boldsymbol{V}$	output vector from the system
V	voltage
$\boldsymbol{X}$	vector of state variables
$\boldsymbol{Z}$	vector of complementary variables to the time derivatives of the states
λ	Boolean parameter indicating the state of a single switch/controlled junction
$\boldsymbol{\Lambda}$	switching law. In this work, it is the diagonal matrix of Boolean functions governing whether a mode of operation is active